Segregation of Chain Ends Is a Weak Contributor to Increased Mobility at Free Polymer Surfaces

Pemra Doruker and Wayne L. Mattice*

Institute of Polymer Science, University of Akron, Akron, Ohio 44325-3909

Received: August 6, 1998; In Final Form: November 9, 1998

Polyethylene thin films are simulated on a high coordination lattice, which is formed by connecting every other site on a diamond lattice. The films present two surfaces to vacuum at 509 K. Each film contains 36 linear or cyclic chains of 50 beads on the coarse-grained lattice, where each bead represents two united-atom carbon atoms. Both linear and cyclic films exhibit bulk density and properties in the interior region, and hyperbolic density profiles at the interfaces. The mobility increases toward the interfaces on the scale of individual beads and chains due to the decrease in density. The increased mobility at the free surfaces is determined more strongly by the low density rather than the segregation of chain ends, since both films exhibit similar characteristics, and there are no chain ends in the film composed of cyclic chains.

Introduction

Near a surface or interface, the properties of polymers may be altered substantially from those observed in the bulk. It is crucial for scientific and technological purposes to determine how and to what extent different surfaces and interfaces will affect the characteristics and, specifically, the mobility of polymer chains. In this respect, several experiments[1−8] have been carried out to determine the mobility of polymer chains at free surfaces by utilizing different techniques and polymeric systems. In most of these studies,[1−5,7,8] the system consists of a thin film supported by a solid surface and the mobility is found to increase, decrease, or stay the same, depending on the interactions at the polymer−solid boundary. Therefore, the results of these systems, where a polymer−solid and a polymer−vacuum boundary coexist, do not give a clear idea of the free surface effect alone. Forrest et al.[6] determined the glass transition temperature of free-standing polystyrene thin films with varying thicknesses. The results showed that the glass transition temperature decreases with decreasing film thickness. Since there are only polymer−vacuum boundaries (on both sides of the film), these experiments[6] clearly indicate that the mobility at the free surface is higher than that of the bulk.

Simulations are useful in this area because they can provide insight on the molecular details of the thin film systems. Mansfield and Theodorou[9] carried out molecular dynamics (MD) simulations of glassy atactic polypropylene thin films. Their results indicated enhanced local mobility at the free surface on the nanosecond time scale. This increased mobility due to the polymer−vacuum interface was apparent at distances into the film that were larger than the radius of gyration of the chains.

We recently performed Monte Carlo (MC) simulations of amorphous polyethylene (PE) thin films on a high coordination lattice and reported results in two parts dealing with the equilibrium and dynamic properties separately.[10,11] The films were composed of linear $C_{100}H_{202}$ chains and had thicknesses of 50−100 Å between the two free surfaces. Reasonable surface energies were obtained for the films. The major findings about the equilibrium (i−iv) and dynamic (v−vi) properties of these films can be summarized as follows. (i) The density profile are hyperbolic, with the end beads being more abundant than the middle beads at the interfaces. (ii) The internal bonds tend to orient parallel to the free surface with the chain ends sticking out toward the vacuum. (iii) The distribution of the chain centers of mass exhibits oscillatory behavior in the direction normal to the surface. (iv) No significant change in the shapes of the chains can be observed across the films. Instead, the chains near the surface orient parallel to the free surface with their largest principal axis lying along the surface. (v) The mobility increases toward the free surfaces at both local and global scales. (vi) The lateral diffusion (parallel to the surfaces) of the chains increases toward the free surfaces. In contrast, chain diffusion in the normal direction to the surfaces slows down due to the confinement of the chains by vacuum.

Although our simulations were performed at 509 K, i.e., well above the glass transition temperature of PE, the finding that the surfaces were more mobile compared to the bulk even at the local scale of individual bonds is consistent with the experimental finding that the glass transition temperature of the thin free-standing film is lower than the bulk.[6] The equilibrium properties of our films were in conformity with results of previous MC simulations on model polymeric systems,[12,13] MD studies of short alkanes,[14] and molecular mechanics simulation of glassy polypropylene films.[15] However, our system sizes and chain lengths are much larger than the atomistic system mentioned above,[14] because we are using an efficient on-lattice MC simulation technique that has been developed for the simulation of specific polymer chains, such as PE. This simulation technique will be described in the next section.

The underlying cause of this lower glass transition temperature has not been established. One cause could be the enrichment of chain ends at the free surface, which has been shown to be true by Mayes using a scaling argument.[16] However, chain end segregation is a more local effect, compared to the increased mobility, which is observed to penetrate deeper into the films from the free surfaces (several radii of gyration). Therefore, in this study, we want to analyze the effect of chain end segregation on the surface properties of thin films by comparing two different films formed by (i) linear and (ii) cyclic

10.1021/jp983308+ CCC: $18.00
Published on Web 12/11/1998

PE chains. Since there are no chain ends in cyclic chains, it will be interesting to compare the equilibrium and dynamic properties of films, composed of linear or cyclic chains.

Simulation Details

A new on-lattice MC simulation technique[17,18] was introduced for the simulation of specific rotational isomeric state (RIS)[19,20] model polymer chains at bulk density. Simulations are performed on a coarse-grained lattice, which is formed by connecting every other lattice site on a diamond lattice. The resulting lattice is identical to the hexagonal packing of hard spheres. However, we prefer to name it as the "second nearest neighbor diamond (2nnd) lattice", to refer to the original diamond lattice, which is a suitable medium for mapping many RIS model chains. Several different polymers, such as PE,[10,11,18,21−24] poly(ethylene oxide),[25] and polypropylene[26] have been mapped and simulated on this coarse-grained lattice so far. References 17 and 18 give details about this high-coordination lattice (coordination number = 12). In the case of mapping PE chains, each lattice site can accommodate a CH_2-CH_2 unit (or a CH_2CH_3 unit at the chain ends).

RIS formalism[19,20] is used to model the short-range interactions on the lattice. These interactions determine the local conformational preferences of specific polymer chains. The original RIS model for PE developed by Abe et al. [27] is modified for the coarse-grained simulations. (see reference 18 for details).

Long-range intra- and intermolecular interactions among nonbonded units are incorporated into the simulations using the Lennard-Jones potential for ethylene units. The second virial coefficient expression is utilized to assign an average interaction energy for each neighboring shell around a lattice site. Reference 21 gives the details for the determination of long-range energies. Self and mutual avoidance is applied to all beads besides long-range interactions. In our simulations of PE thin films, we consistently use the parameter set II in reference 10, which is found to produce reasonable density in the bulk region of the films. This specific parameter set uses the average interaction energies for the first three shells as 14.122, 0.526, and −0.627 kJ/mol, sequentially.[10] It is possible to perform thin film simulations on the 2nnd lattice because the third shell interactions are attractive, i.e., they bring cohesion to the system.

It is also possible to reverse-map any coarse-grained snapshot back to the atomistic model in continuous space during the course of the simulation. This is achieved by placing the missing atoms on the lattice and performing a brief energy minimization of the system. Thus, large bulk and film systems of PE were equilibrated efficiently in order to analyze atomistic system properties,[10,22] which were in agreement with experimental results.

Single bead moves are applied in the simulations, where each move corresponds to the displacement of two or three backbone atoms on the fully atomistic chain. Each Monte Carlo step (MCS) corresponds to a series of single bead moves, during which all the beads in the system are randomly attempted for movement. Reference 22 gives the details on the different kind of single bead moves performed. Since only local moves are allowed in the simulations, the dynamic properties of bulk PE systems were found to be satisfactory,[24] when compared with the MD results of similar atomistic systems.[28]

In our current study, PE chains are made of 50 coarse-grained beads (CH_2CH_2 units), which correspond to linear $C_{100}H_{202}$ chains (or $C_{100}H_{200}$ in the case of cyclic chains) after reverse mapping. The films, which present two surfaces to vacuum, consist of 36 chains in total. In the following discussions, the films will be differentiated as (i) F-LIN, having 36 linear chains, and (ii) F-CYC, having 36 cyclic chains. Both systems are simulated at 509 K. The periodic cross-sectional area of all films in the X and Y directions is 2501 Å^2 (21 × 22 lattice sites with 2.5 Å lattice spacing). The film thickness in the Z direction (normal to the free surfaces) varies a little bit according to the system composition, since the system chooses its own bulk density due to cohesive long-range interactions. F-CYC has a slightly higher density (and smaller thickness) than F-LIN. Simulations are performed for 2×10^6 MCS after equilibration periods of $(2-3) \times 10^6$ MCS. Thin films are formed starting from equilibrated bulk snapshots and increasing one of the periodic sides of the system to infinity using the method of Misra et al.[29]

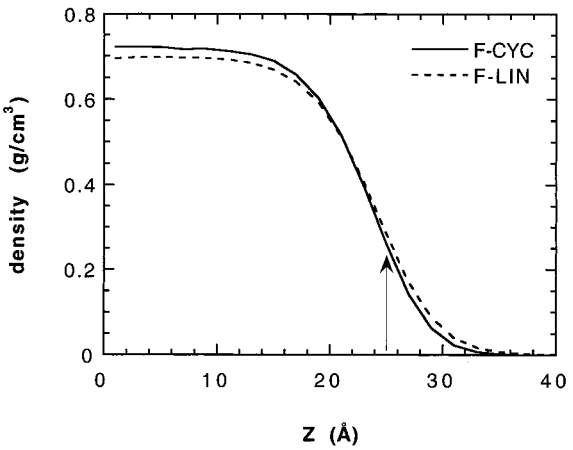

Figure 1. Density profiles of two free-standing films (F-CYC and F-LIN) from the center of mass of the film in the Z direction, which is normal to the free surfaces. The arrow on the figure is explained in the section on dynamic properties.

Results and Discussion

Density profiles. Figure 1 compares the density profiles of F-LIN and F-CYC as a function of the Z direction, which is perpendicular to the film surfaces. $Z = 0$ corresponds to the film center of mass in this specific direction. Averaging is performed for the two sides of the film due to symmetry. Although the two profiles look similar, the bulk density in the interior of the film formed by cyclic chains is slightly higher than that of linear chains and the interfacial region is slightly narrower. The small differences in the two films indicate that the local packing of cyclic chains is more efficient compared to that of linear chains, due to the inefficient packing of chain ends in F-LIN.

The density profiles at the interface can be fitted to the following hyperbolic tangent function[30]

$$\rho(Z) = \frac{\rho_B}{2}\left[1 - \tanh\left(\frac{Z}{\xi}\right)\right] \quad (1)$$

where ρ_B is the bulk density of the films. The correlation length ξ is found to be 5.23 Å for F-CYC and 5.44 Å for F-LIN. According to these curve fits, the interfacial thicknesses of F-CYC and F-LIN are 11.5 and 12.0 Å, respectively, when interfacial thickness is defined as the distance over which the density of the film decreases from 90% to 10% of its bulk value.

Orientation of Bonds. The orientational order parameter, which is defined as

$$S = \frac{1}{2}\langle 3(\cos^2\theta) - 1\rangle \quad (2)$$

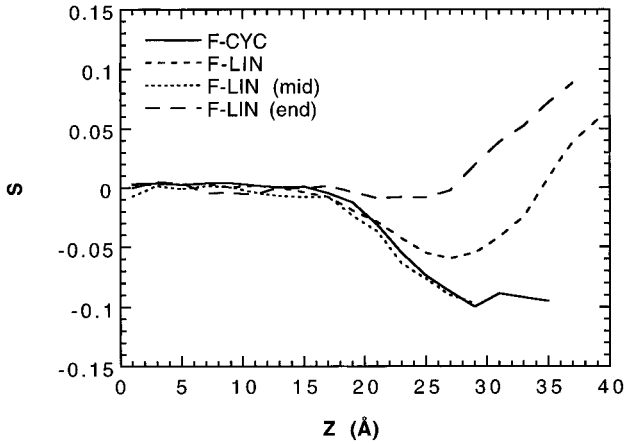

Figure 2. Orientation of the coarse-grained bonds with the *Z* axis (see text for definition) for all the bonds in F-CYC (solid line) and F-LIN (short dashed) and for the middle (dotted) and end (long dashed) bonds in F-LIN.

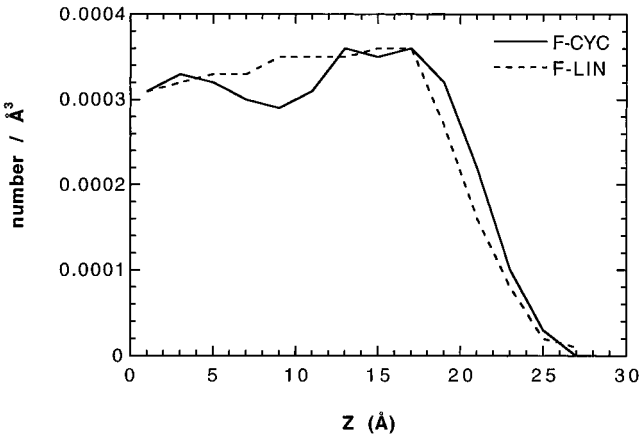

Figure 3. Center of mass distribution of the chains across the two films. The number of chains in 2 Å bins is divided by the volume of the bin.

is used to determine any orientation preferences of the bonds across the film. In this definition, θ is the angle between any coarse-grained 2nnd bond and the normal direction to the surfaces, i.e., the *Z* axis. According to this definition, $S = 0$, -0.5, and 1.0 represent random, perfect parallel and perfect perpendicular orientations, respectively.

Figure 2 displays *S* as a function of the *Z* coordinate for all bonds of films F-LIN and F-CYC, represented by short-dashed and solid lines, respectively. The dotted and long-dashed lines represent the order parameter for the middle and end bonds of F-LIN, respectively. All of the order parameters are very close to zero near the midplane of the film. Different behavior is seen in the surface region, where the density decreases. The order parameter for the middle bonds of the linear chains exhibits almost the same behavior as that of cyclic chains, i.e., a tendency to orient parallel to the surfaces in the region of low density. In contrast, the end bonds in this region tend to stick out of the surfaces and orient perpendicular to the surfaces. The tendency for segregation of end bonds in the very low density region of F-LIN causes *S* to become positive at the edge of this film, in contrast to the result for F-CYC. The differences in the structure of the surface region of the two films are more apparent in the behavior of *S* than in the behavior of the density.

Chain Properties. Here, we compare the global equilibrium properties of the chains. The centers of mass distribution of the chains, expressed as the number of chains per volume of bin, are shown in Figure 3 for films F-LIN and F-CYC. The oscillatory behavior of the distribution is more clearly observed in the case of cyclic chains, since the radius of gyration of cyclic chains ($\langle R_g^2 \rangle = 94$ Å^2) is much smaller than that for linear ones ($\langle R_g^2 \rangle = 180$ Å^2). In the case of linear chains, the same behavior was observed with a larger period in previous simulations of a thicker film.[10]

The eigenvalues ($L_1^2 > L_2^2 > L_3^2$) of the radius of gyration tensor of each chain are calculated by converting to the principal axis system. Figure 4a gives the three eigenvalues (principal moments) of the chains as a function of the *Z* coordinate. There is no dependence of the eigenvalues on the position within the film. Figure 4b gives the orientation of the first and third principal axis of the chains (corresponding to L_1 and L_3) with the *Z* axis, as defined by the order parameter *S* (eq 2). The chains are randomly oriented in the bulk region. Toward the interface, the chains reorient by aligning their first (longest) principal axis parallel to the interface. These orientation preferences, which

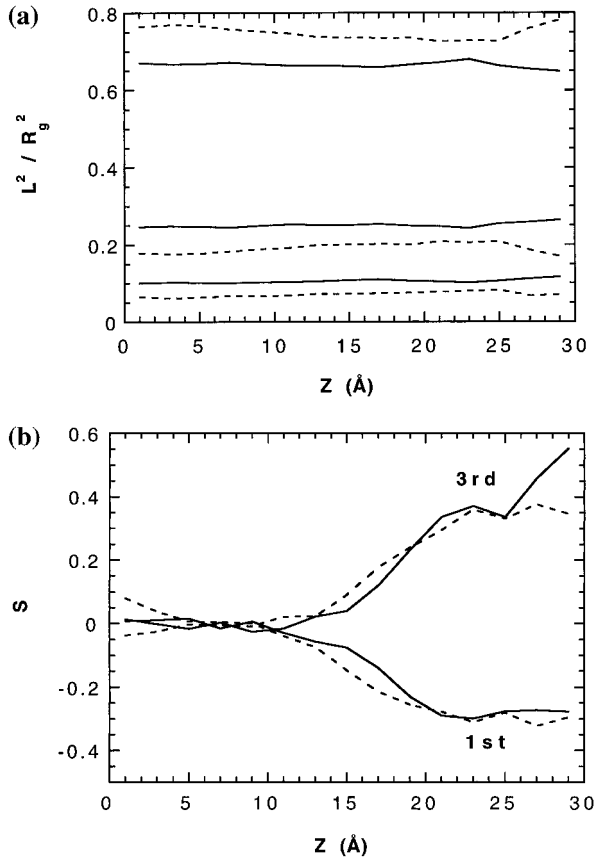

Figure 4. (a) Principal moments of the radius of gyration tensor of chains (divided by the squared radius of gyration) as a function of the *Z* coordinate in F-CYC (dashed lines) and F-LIN (solid lines). (b) Orientation of the first (longest) and third principal axis of the chains with the *Z* axis, as a function of the *Z* coordinate in F-CYC (dashed lines) and F-LIN (solid lines).

were previously observed for linear chains,[10] seem to be pertinent in the case of cyclic chains too.

Surface Energies. Figure 5a gives the total energy (per bead) and its components, i.e., the short-range intramolecular (from the RIS model) and the long-range intermolecular energies as a function of the *Z* coordinate for F-CYC. All energies are extracted directly from the coarse-grained simulation results. The difference between the distributions of F-CYC and F-LIN (Figure 7a in reference 10) is in the short-range energies, which are shown in Figure 5b. In the interfacial region, the short-

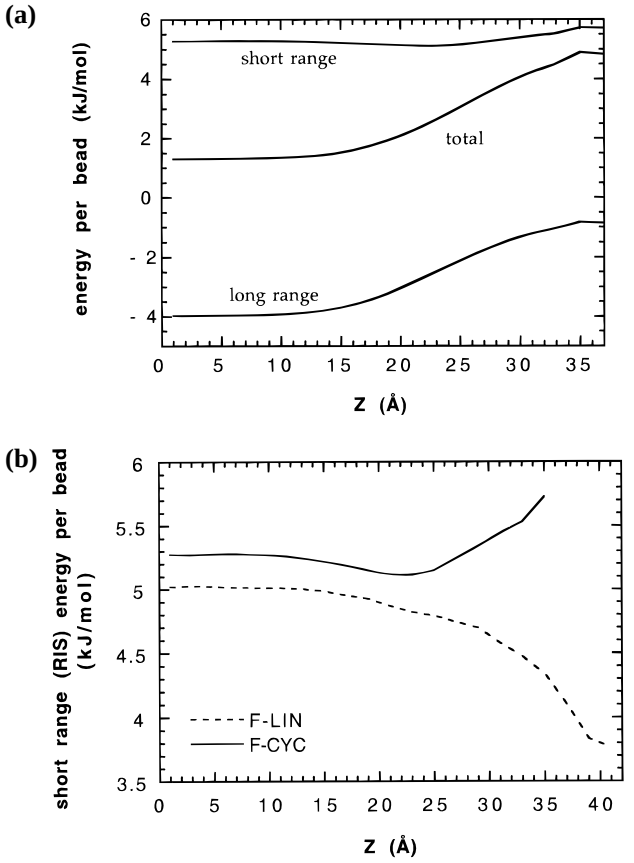

Figure 5. (a) Average short- and long-range and total energies per bead as a function of the *Z* coordinate for F-CYC. (b) Comparison of short-range (RIS) energies per bead for F-CYC and F-LIN, as a function of *Z*.

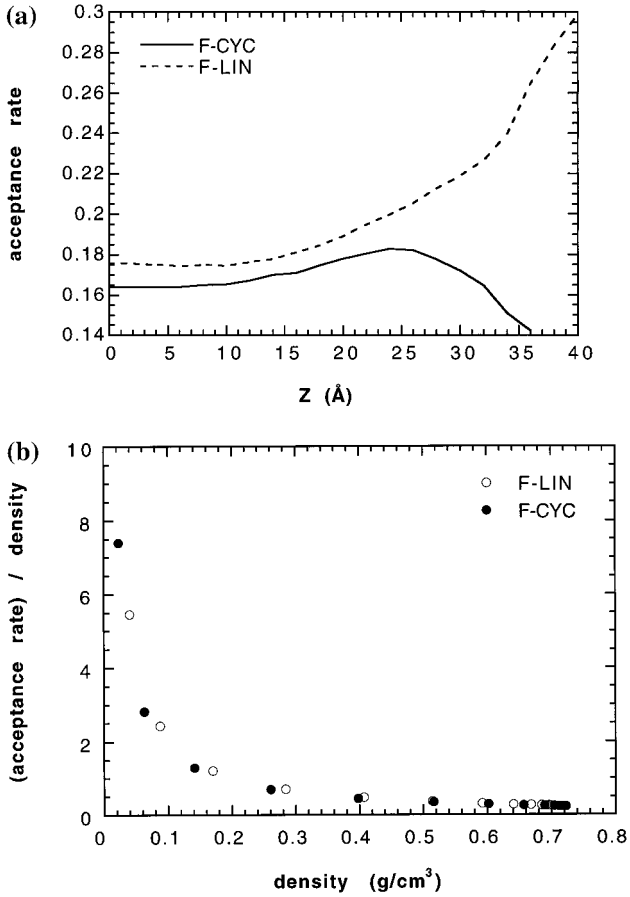

Figure 6. (a) Acceptance rate of single-bead MC moves as a function of *Z*. (b) Acceptance rate divided by density as a function of density for both films.

range energy per bead drops constantly in F-LIN, whereas in F-CYC the short-range energy per bead increases after an initial slight decrease. The reason for this may be the fact that linear chains can adopt more conformations than cyclic chains at the lower density portion of the interface, due to the flexibility of chain ends.

Surface energy can be calculated using the relationship

$$\gamma = \frac{\langle E_{2D}\rangle - \langle E_{3D}\rangle}{2A} \tag{3}$$

where $\langle E_{2D}\rangle$ and $\langle E_{3D}\rangle$ denote the average film and bulk potential energies, respectively, and $2A$ gives the total surface area of the interfaces. It may be possible to extract an average bulk energy from the bulk region of the thin film simulations, as described in reference 10. The problem with 36-chain films is that their bulk region is too thin, so the results will just be rough estimates. Surface energies of 21 and 22 erg/cm^2 are calculated for F-LIN and F-CYC, respectively. (In previous work, 22.2 erg/cm^2 was found for the thicker linear film.[10]) The difference in the density profiles (Figure 1) for F-LIN and F-CYC is consistent with F-CYC having a slightly higher surface energy than F-LIN.

Dynamic Properties. Comparison of F-LIN and F-CYC in the previous section shows that both films exhibit quite similar equilibrium properties with regard to density profile, orientation of radii of gyration tensor, and surface energy, but the chain ends produce a difference in local structure (order parameter for bonds). We now inquire whether the special dynamics at the surface is controlled by properties that the two films have in common (do the two films have similar dynamics?) or by properties that are different in the two films (do they have different dynamics?). In this section, we will summarize the findings on the dynamics of F-CYC, which also conform qualitatively with the previous results on the linear system (F-LIN).[11]

(1) The acceptance rates of the single bead MC moves are shown as a function of the *Z* coordinate in Figure 6a. The acceptance rate increases toward the free surfaces in the interfacial region of both films up to a specific point, which is indicated by the arrow on density profiles in Figure 1 (at $Z \approx$ 25 Å). This increase mainly results from the increase in free volume, since in this region the density decreases almost to $\rho_B/3$ (one-third of the bulk density). Toward the vacuum side of this point, i.e., in the lower density region, the acceptance rates of the two films exhibit quite different characteristics. The local mobility of F-CYC decreases in this region, which might be attributed to the energy penalty against the movement of the beads out into vacuum. In the case of the F-LIN film, the local mobility is enhanced in this low-density region, even though the same energy penalty exists. This should result from the presence of the end beads, which can waggle freely unlike the middle beads in F-CYC film, which must retain connectivity with two bonded neighbors.

The total acceptance rate of the F-CYC film is 0.17, which is slightly higher compared to that of its bulk region acceptance of 0.164. Therefore, the increase up to $Z \approx 25$ Å seems to be more important than the slow down beyond this point. For the F-LIN film, the total and bulk acceptance rates are 0.181 and 0.175. It is interesting to note that Figure 6a shows just the opposite trend of Figure 5b. Figure 6b displays the acceptance

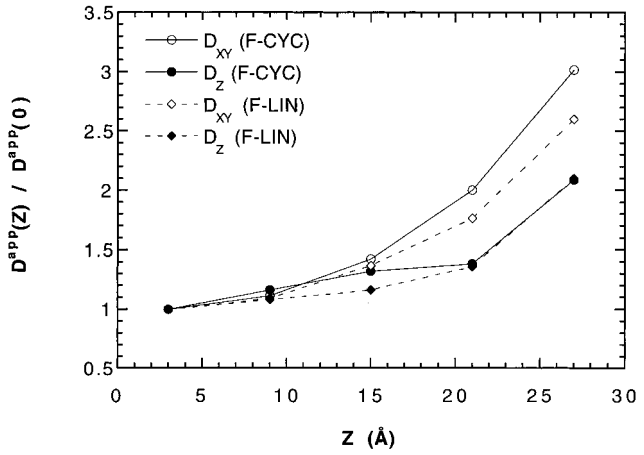

Figure 7. The relative apparent diffusivity, $D^{app}(Z)/D^{app}(0)$, as a function Z in different bins across the F-CYC and F-LIN films, calculated at 5000 MCS. D_{XY} and D_Z represent the diffusion coefficients in the parallel and normal directions to the surfaces.

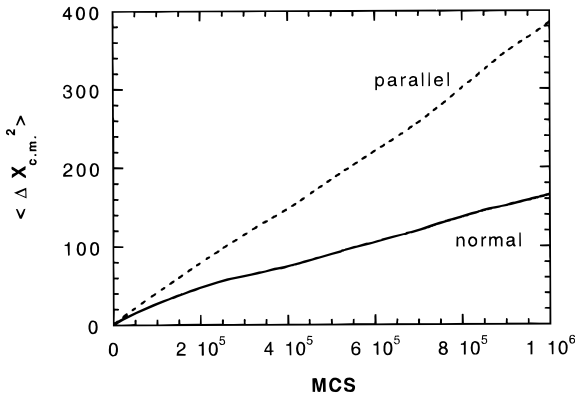

Figure 8. The squared center of mass displacement of the chains as a function of time, i.e., MCS for F-CYC. The components of diffusion in the directions that are parallel and normal to the free surfaces are indicated separately.

rate divided by the density vs density for both films. In this plot, no difference could be observed between the trends of F-CYC and F-LIN.

(2) The short-time apparent diffusion coefficient[31] in the Z direction is defined as

$$D_Z^{app} = \frac{1}{2t_f}\langle [Z_{cm}(t + t_f) - Z_{cm}(t)]^2 \rangle \qquad (4)$$

where Z_{cm} is the Z coordinate of the chain center of mass and t_f is an arbitrary final time. Figure 7 gives the relative increase in the apparent diffusion coefficients, $D^{app}(Z)/D^{app}(0)$, as a function of the Z coordinate for F-CYC and F-LIN, where $D^{app}(0)$ stands for the bulk value at $Z = 0$. D_{XY} and D_Z represent the diffusion coefficients in the parallel and normal directions to the surfaces. D_{XY} is calculated by averaging over the center of mass displacements in the X and Y directions. Here, t_f = 5000 MCS, which is a time period that is short enough so that most of the chains stay in their original bins. The relative increase in both components of diffusion toward the interfaces is similar in the two films.

(3) Figure 8 displays the squared center of mass displacement of all the chains in the F-CYC film on a longer time scale. The parallel and normal components are distinguished on this plot. The diffusion of the chains in the normal direction is lower compared to the parallel direction due to the confinement of the chains between the free surfaces, i.e., vacuum. The same behavior was observed in the case of linear chains.[11] In the long-time limit, the diffusion in the normal direction will saturate to a constant value due to confinement.

The diffusion coefficients, evaluated by a linear fit to the data between 4×10^5 and 10^6 MCS, are reported in Å^2/MCS as follows:

$$D_{XY} = 0.000\ 20 \text{ (F-CYC)}$$

$$D_{XY} = 0.000\ 25 \text{ (F-LIN)}$$

$$D_Z = 0.000\ 08 \text{ (F-CYC)}$$

$$D_Z = 0.000\ 07 \text{ (F-LIN)}$$

Conclusion

Two regions can be identified at the interface of thin films, when a comparison is performed among the local mobility of films composed of primarily linear $C_{100}H_{202}$ and cyclic $C_{100}H_{200}$. Both films experience similar increases in mobility in the interfacial region up to the point where the bulk density decreases to $\rho_B/3$. Beyond this point, toward the vacuum side, the mobility of F-LIN continues to increase whereas that of F-CYC starts to decrease. In this region of the interface, the enhancement of mobility due to the end beads can be observed.

The simulations were performed with chains that have ends that are indistinguishable from the beads in the interior. Different behavior might be obtained if the end beads were labeled so that they were different from the internal monomers.[32]

Acknowledgment. This work is supported by National Science Foundation, Grant DMR 95-23278.

References and Notes

(1) Keddie, J. L.; Jones, R. A. L.; Cory, R. A. *Europhys. Lett.* **1994**, *27*, 59.
(2) Zheng, X.; Sauer, B. B.; van Alsten, J. G.; Schwartz, S. A.; Rafailovich; M. H.; Sokolov, J.; Rubenstein, M. *Phys. Rev. Lett.* **1995**, *74*, 407.
(3) Xie, L.; DeMaggio, G. B.; Frieze, W. E.; DeVries, J.; Gidley, D. W.; Hristov, H. A.; Yee, A. F. *Phys. Rev. Lett.* **1995**, *74*, 4947.
(4) Tanaka, K.; Taura, A.; Ge, S.; Takahara, A.; Kajiyama, T. *Macromolecules* **1996**, *29*, 3040.
(5) Frank, B.; Gast, A. P.; Russell, T. P.; Brown, H. R.; Hawker, C. *Macromolecules* **1996**, *29*, 6531.
(6) Forrest, J. A.; Dalnoki-Veress, K.; Stevens, J. R.; Dutcher, J. R. *Phys. Rev. Lett.* **1996**, *77*, 2002.
(7) Kajiyama, T.; Tanaka, K.; Takahara, A. *Macromolecules* **1997**, *30*, 280.
(8) Liu, Y.; Russell, T. P.; Samant, M. G.; Stöhr, J.; Brown, H. R.; Cossy-Favre, A.; Diaz, J. *Macromolecules* **1997**, *30*, 7768.
(9) Mansfield, K. F.; Theodorou, D. N. *Macromolecules* **1991**, *24*, 6283.
(10) Doruker, P.; Mattice, W. L. *Macromolecules* **1998**, *31*, 1418.
(11) Doruker, P.; Mattice, W. L. *Macromolecules*, in press.
(12) Madden, W. G. *J. Chem. Phys.* **1987**, *87*, 1405.
(13) Kumar, S. K.; Russell, T. P.; Hariharan, A. *Chem. Eng. Sci.* **1994**, *49*, 2899.
(14) Harris, J. G. *J. Phys. Chem.* **1992**, *96*, 5077.
(15) Mansfield, K. F.; Theodorou, D. N. *Macromolecules* **1990**, *23*, 4430.
(16) Mayes, A. M. *Macromolecules* **1994**, *27*, 3114.
(17) Rapold, R. F.; Mattice, W. L. *J. Chem. Soc., Faraday Trans.* **1995**, *91*, 2435.
(18) Rapold, R. F.; Mattice, W. L. *Macromolecules* **1996**, *29*, 2457.
(19) Flory, P. J. *Statistical Mechanics of Chain Molecules*; Wiley: New York, 1969.
(20) Mattice, W. L.; Suter, U. W. *Conformational Theory of Large Molecules. The Rotational Isomeric State Model in Macromolecular Systems*; Wiley: New York, 1994.
(21) Cho, J.; Mattice, W. L. *Macromolecules* **1997**, *30*, 637.
(22) Doruker, P.; Mattice, W. L. *Macromolecules* **1997**, *30*, 5520.

(23) Bahar, I.; Cho, J.; Erman, B.; Haliloglu, T.; Kim, E.-G.; Mattice, W. L.; Monnerie, L.; Rapold, R. F. *Trends Polym. Sci.* **1997**, 5, 155.
(24) Doruker, P.; Mattice, W. L. *Macromol. Sym.* **1998**, *133*, 47.
(25) Doruker, P.; Rapold, R. F.; Mattice, W. L. *J. Chem. Phys.* **1996**, *104*, 8742.
(26) Haliloglu, T.; Mattice, W. L. *J. Chem. Phys.* **1998**, *108*, 6989.
(27) Abe, A.; Jernigan, R. L.; Flory, P. J. *J. Am. Chem. Soc.* **1966**, *88*, 631.
(28) Paul, W.; Smith, G. D.; Yoon, D. Y. *Macromolecules* **1997**, *30*, 7773.
(29) Misra, S.; Fleming, P. D., III; Mattice, W. L. *J. Comput.-Aided Mater. Des.* **1995**, *2*, 101.
(30) Kumar, S. K.; Russell, T. P.; Hariharan, A. *Chem. Eng. Sci.* **1994**, *49*, 2899.
(31) Yoon, D. Y.; Vacatello, M.; Smith, G. D. In *Monte Carlo and Molecular Dynamics Simulations in Polymer Science*; Binder, K., Ed.; Oxford University Press: New York, 1995; p 433.
(32) Tanaka, K.; Jiang, X.; Nakamura, K.; Takahara, A.; Kajiyama, T.; Ishizone, T.; Hirao, A.; Nakahama, S. *Macromolecules* **1998**, *31*, 5148.